Trilayered MoS_2 Metal–Semiconductor–Metal Photodetectors: Photogain and Radiation Resistance

Dung-Sheng Tsai, Der-Hsien Lien, Meng-Lin Tsai, Sheng-Han Su, Kuan-Ming Chen, Jr-Jian Ke, Yueh-Chung Yu, Lain-Jong Li, and Jr-Hau He, *Senior Member, IEEE*

***Abstract*—Trilayered MoS_2 metal–semiconductor–metal (MSM) photodetectors (PDs) exhibit the photogain is up to 24 with high responsivity ($\sim$1.04 A/W). This is because photocarriers generated at the MoS2 between two Au electrodes drift toward the metal–semiconductor interfaces due to band bending under applied bias and are then trapped at the surface state sites at the Au/MoS2 interfaces, giving rise to the decrease in Schottky barrier height. Moreover, MoS_2 MSM PDs show fast operation speed; as the contact spacing reduces from 8 to 4 μm, the rise time and fall time of PDs reduce from 70 to 40 μs and from 110 to 50 μs, respectively. Trilayered MoS_2 MSM PDs can operate even after 2-MeV proton illumination with $\sim 10^{11}$ cm^{-2} fluences, indicating the high radiation tolerance. This work demonstrates that trilayer MoS_2 opens up a new dimension for 2-D nanomaterial applications in harsh electronics.**

***Index Terms*—Graphene, harsh environment, MoS_2, photodetector, radiation resistance.**

I. Introduction

TWO-dimensional (2-D) materials with rich physical phenomena, such as the existence of quantum confinements and the lack of interlayer interactions, allow us to develop More-than-Moore, more flexible and more efficient electronic/optoelectronic devices in the future [1]–[5]. Among a variety of 2-D nanomaterials, graphene is attractive for optoelectronic applications due to its broadband absorption, high carrier mobility, and short carrier lifetime [6]. However, owing to the absence of a bandgap, the photogeneration carrier is only extracted by the local potential near the metal–graphene interface, differing from that of semiconductor PDs [7]. Therefore, even though the ultrafast response speed have been demonstrated, the responsivity of the pristine graphene PDs is still low due to the limited absorption caused by the small effective detection areas, hindering practical applications [8]–[11]. Accordingly, how to enhance the responsivity of graphene-based PDs *via* combining with new semiconducting materials and utilizing novel physical concepts (such as exploiting nanoparticles, plasmonic nanostructures, and microcavities) has been a major concern recently [12]–[15]. However, the responsivity of graphene-based PDs is still limited as the photogain is smaller than unity. Until recently, by employing photogating effect, the hybrid grapheme-quantum dot PDs exhibits the responsivity of $\sim 10^7$ A/W due to the ultrahigh photogain of $\sim 10^8$, which is not achievable for the pristine graphene [12].

Layered MoS_2, a newly 2-D nanomaterial with a direct, finite bandgap, provides a possible solution to overcome the drawbacks of pristine graphene [16]–[21]. The indirect bandgap of 1.2 eV for bulk MoS_2 transforms to the direct bandgap of 1.9 eV for layered MoS_2 because of a quantum confinement effect [16]–[20], opening the many possibilities of optoelectronic applications, such as PDs [22], [23], solar cells [24], and solid-state lighting [25] with lightweight and ultrathin materials. Recently, as compared to that obtained from the pristine graphene ($\sim 1 \times 10^{-3}$A/W) [7], [8], the high photoresponsivity (7.5×10^{-3}A/W) from the MoS_2 phototransistors has been obtained due to direct bandgap absorption [26].

Space electronics and optoelectronics have a long history of power and system failures/resets due to long-duration radiation exposures, unpredictable solar proton activity, and ambient galactic cosmic ray environment, leading to undesirable operation failures [27]. Moreover, it is known that the solar flare activity is periodically changed and expected to peak between 2013 and 2014. As the satellites stuffed with a variety of electronic and optoelectronic devices may suffer from the illumination of high-energy protons, ions, ultraviolet radiation, and other energetic particles, many experts concentrate their efforts to prevent the disruptions on communications, navigation, and other vital networks caused by the system/device failures. Furthermore, the development of space electronics and optoelectronics has particular challenges because they are constrained by severe cost and weight restrictions [28]. Therefore, it is demanded to develop ultralightweight and ultrathin electronic/optoelectronic devices with high radiation resistance.

Manuscript received April 1, 2013; revised May 11, 2013 and June 5, 2013; accepted June 9, 2013. Date of publication July 9, 2013; date of current version August 14, 2013. This work was supported by in part by the National Science Council of Taiwan under Grant 99-2622-E-002-019-CC3, Grant 99-2112-M-002-024-MY3, and Grant 99-2120-M-007-011 and in part by the National Taiwan University (10R70823). The work of L.-J. Li was supported by the Academia Sinica (IAMS and Nano program).

D.-S. Tsai, D.-H. Lien, M.-L. Tsai, J.-J. Ke, and J.-H. He are with the Department of Electrical Engineering, and Graduate Institute of Photonics and Optoelectronics, National Taiwan University, Taipei 10617, Taiwan (e-mail: jhhe@cc.ee.ntu.edu.tw).

S.-H. Su is with the Department of Electrical Engineering, and Graduate Institute of Photonics and Optoelectronics, National Taiwan University, Taipei 10617, Taiwan and also with the Institute of Atomic and Molecular Sciences, Academia Sinica, Taipei 10617, Taiwan.

K.-M. Chen and Y.-C. Yu are with the Institute of Physics, Academia Sinica, Taipei 11529, Taiwan.

L.-J. Li is with the Institute of Atomic and Molecular Sciences, Academia Sinica, Taipei 10617, Taiwan.

Color versions of one or more of the figures in this paper are available online at http://ieeexplore.ieee.org.

Digital Object Identifier 10.1109/JSTQE.2013.2268383

In this study, trilayered MoS_2 metal–semiconductor–metal (MSM) PDs with a photogain/responsivity up to 24/1.04 (A/W) and high radiation resistance (up to $\sim 10^{11}$ cm^{-2} of 2-MeV proton fluences) for harsh environment applications have been developed. Due to the Schottky barrier lowering effect induced by the photocarriers generated at the MoS2 between two Au electrodes and trapped at surface states in the MoS_2/Au contact interfaces, photogain is greater than unity, leading to high responsivity. In addition, the fast response times/recovery times from 70/110 to 40/50 μs have been demonstrated as the contact spacing is reduced from 8 to 4 μm. The excellent optical properties of trilayered MoS_2 demonstrated for extreme environments for the first time promise a new generation of fast, thin, and lightweight PDs based on 2-D nanomaterials for harsh electronics and optoelectronics, such as sensing, imaging, and intrachip optical interconnects in space.

II. Experiment

For the preparation of trilayered MoS_2, 0.25-g $(NH_4)_2MoS_4$ (Alfa Aesar, purity of 99.99%) was added to 20 mL DMF to form a 1.25 wt% solution. It was sonicated for 20 min to achieve a homogenous $(NH_4)_2MoS_4$ solution. The sapphire substrates were cleaned with a Piranha solution ($H_2SO_4/H_2O_2 = 7/3$) to remove the surface contaminants. The cleaned substrates were immersed into the $(NH_4)_2MoS_4$ solution, followed by slow pulling-up (0.5 mm/s). After that, the substrates were baked on a hot plate at 120 °C for 30 min until the majority of solvent molecules were evaporated. The substrate was then placed in the edge of a quartz tube with a flow of H_2 (20 sccm) and Ar (80 sccm). When the temperature in the center of the furnace reached 500 °C, the substrate was moved to the center of the furnace. Sixty minutes later, the sample was cooled down to room temperature under H_2/Ar ambient by putting the sample back to the tube edge. The sample was moved to the furnace center again for the second postannealing when the center of the furnace reached 1000 °C in an Ar^+ sulfur environment at 500 torr. After the MoS_2 layers were grown on sapphire substrates, we transferred the MoS_2 layers onto freshly cleaned SiO_2/Si substrates for fabricating MSM PDs.

The MSM PDs adopted Au electrodes with interdigitated fingers on MoS_2/SiO_2/Si substrates. The 100-nm-thick Au fingers were designed to be 8 μm wide and 150 μm long with 8-μm-wide spacing and deposited by electron beam evaporation to serve as Schottky contacts. The MoS_2 MSM PDs were measured under 532-nm laser illumination (the beam diameter is $\sim$1 mm) in air.

After the fabrication process of MoS_2 MSM Schottky PDs, Raman spectra were obtained by confocal Raman microscopy systems (NT-MDT) with a 473-nm laser (the spot size of laser is $\sim$0.5 μm in diameter). Field-emission transmission electron microscopy (TEM) (JEOL JEM-2100 F, operated at 200 kV with a point-to-point resolution of 0.19 nm) was used to investigate the microstructures. The samples for TEM observation were prepared using lacy-carbon Cu grid to scratch the surface of MoS_2 samples. The Keithley 4200-SCS semiconductor characterization system was used to measure *I–V* characteristics and

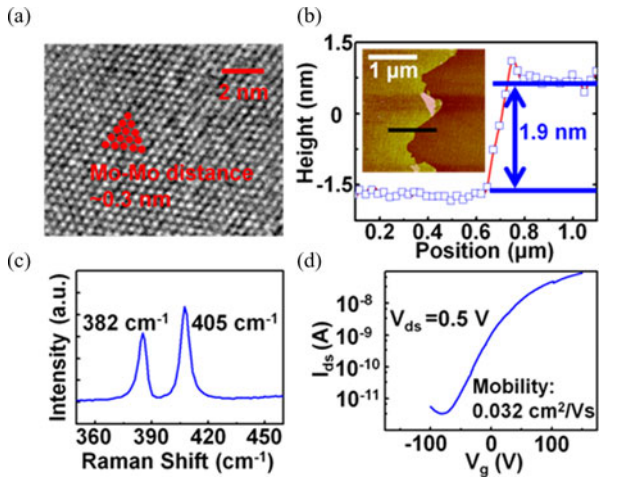

Fig. 1. (a) The high-resolution TEM image for the trilayered MoS_2. (b) AFM image and thickness of trilayered MoS_2. (c) Raman spectrum of trilayered MoS_2 under ambient conditions at room temperature. (d) The typical transfer curves [conductivity versus gate voltage (V_g)] for trilayered MoS_2 field-effect transistors.

responsivity of the trilayered MoS_2 PDs. Moreover, for radiation resistance testing, MoS_2 MSM PDs were irradiated with a 2 MeV proton beam with the fluences ranging from 10^{10} to 10^{12} cm^{-2} from a 3 MV tandem accelerator (NEC 9SDH-2, National Electrostatics Corporation).

III. Results and Discussion

The optimized fabrication process used here is able to produce very homogeneous MoS_2 trilayers across the whole sample. In general, the more diluted precursor solution and faster dip-coating result in a thinner MoS_2 layer. Here, we aim at large-area and superior-quality trilayered MoS_2 for PD applications. More details about the two-step thermolysis process can be found elsewhere [19]. As shown in Fig. 1(a), periodic Mo atoms (with distance of $\sim$0.3 nm) arranging in hexagonal symmetry is observed in the high-resolution TEM image, indicating the crystallinity of the MoS_2 layers. A line scan of atomic force microscopy (AFM) in Fig. 1(b) reveals the edge of the thin MoS_2 layers with a distinct step of $\sim$1.9 nm, corresponding to three MoS_2 layers (the thickness of each layer: $\sim$0.65 nm) [19]. The Raman characteristic peaks at 382 and 405 cm^{-1} correspond to E^1_{2g} and A_{1g} modes of MoS_2, respectively, as shown in Fig. 1(c) [19], [20].

The peak frequency difference Δ between E^1_{2g} and A_{1g} Raman peaks (i.e., 382 and 405 cm^{-1}) has been found to relate to the number of MoS_2 layers. The value of Δ ($\sim$23 cm^{-1}) evidences the existence of trilayered MoS_2 films [19]. Moreover, in order to evaluate the electrical performance of trilayered MoS_2, the field-effect mobility of electrons ($\sim$0.03 cm^2 V^{-1} S^{-1}) was extracted based on the slope $\Delta I_d/\Delta V_g$ fitted to the linear regime of the transfer curves using the equation

$$\mu = (L/WC_{\rm ox}V_d)\,(\Delta I_d/\Delta V_g) \tag{1}$$

where L and W are the channel length and width, and $C_{\rm ox}$ is the gate capacitance, as shown in Fig. 1(d) [19].

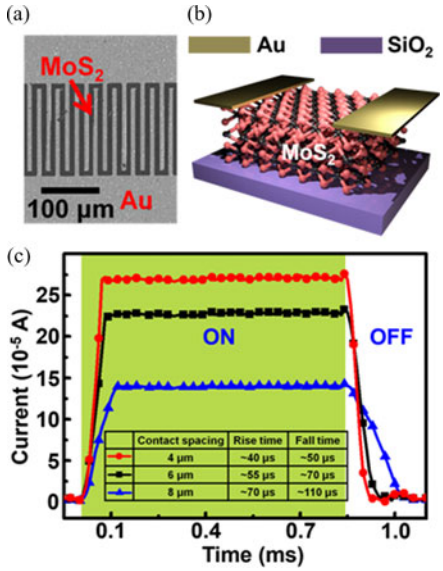

Fig. 2. (a) The top-view optical microscopic image of the MoS_2 MSM PDs with interdigitated electrodes. (b) The schematic of MoS_2 MSM PDs. (c) The time response of MoS_2 MSM PDs with different contact spacing (i.e., 4, 6, and 8 μm) measured at 5 V bias with $I_{\text{light}} = 2.0 \times 10^4$ W/m^2. The inset is the table of contact spacing-dependent rise and fall times extracted from (c).

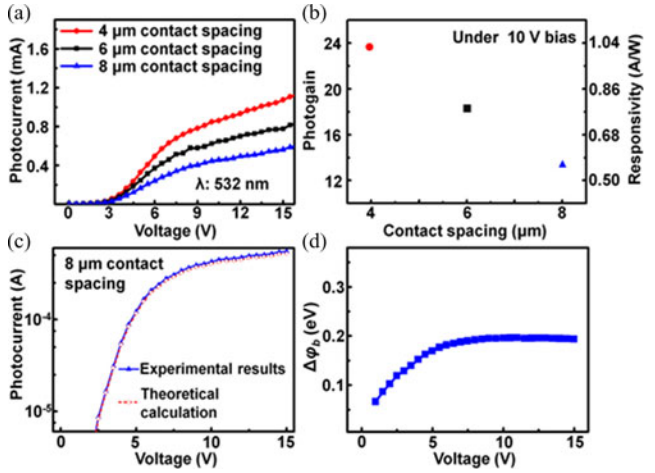

Fig. 3. (a) *I–V* curves of MoS_2 MSM PDs with different contact spacing (i.e., 4, 6, and 8 μm) measured under 532-nm light illumination ($I_{\text{light}} = 2.0 \times 10^4$ W/m^2). (b) The photogain as a function of contact spacing measured under 10 V bias and 532-nm light illumination ($I_{\text{light}} = 2.0 \times 10^4$ W/m^2). (c) The experimental and theoretical *I–V* curves of MoS_2 MSM PDs. (d) The Schottky barrier height reduction as a function of applied bias.

In order to demonstrate the photosensitivity of trilayered MoS_2, the devices were fabricated in MSM geometry with Au Schottky contacts to MoS_2 [as shown in the top-view optical microscopic image and the schematic in Fig. 2(a) and (b)] to effectively lower the dark current. Fig. 2(c) presents the photocurrent of MoS_2 PDs with 8, 6, and 4-μm contact spacing as a function of time under 532-nm illumination (light intensity $I_{\text{light}} = 2.0 \times 10^4$ W/m^2) under 5 V bias. Under illumination, the current rises to a high value (ON state), and then returns to a low value when the light is OFF (OFF state). The transition between ON and OFF states reveals the response/recovery speed of the MoS_2 PDs. The results are shown in Fig. 2(c), from which rise time (from 10% to 90% of the maximum photocurrent as switching light from OFF to ON)/fall time (from 90% to 10% of the maximum photocurrent as switching light from ON to OFF) of MoS_2 MSM PDs can be decreased from 70/110 to 40/50 μs as the contact spacing is decreased from 8 to 4 μm. This indicates that the shorter transition time of photocarriers results from 1) the smaller contact spacing and 2) the higher electric field as decreasing contact spacing under the same applied bias [29].

In addition to improving the operation speed, it is suggested that by diminishing the spacing of interdigitated electrodes the detector can enhance the responsivity [29]. Accordingly, in addition to the contact spacing-dependent photoresponse time, the contact spacing-dependent photocurrent of MoS_2 MSM PDs has been investigated and shown in Fig. 3(a). The *I–V* curves of MoS_2 PDs with 8, 6, and 4-μm contact spacing were measured under 532-nm light illumination ($I_{\text{light}} = 2.0 \times 10^4$ W/m^2), indicating that the photocurrent is increased as the electrode contact spacing is shrunk. The absorption coefficient of few-layered MoS_2 is up to $\sim 7.5 \times 10^5$ cm^{-1}, indicating that few-layered MoS_2 can absorb ~10–15% of incident light in the visible wavelength region [18], [23]. Accordingly, the photogain of the MoS_2 PD can be further estimated by

$$R = I_p/P = \eta_{\text{ext}} G q/hv \tag{2}$$

where R is the responsivity, I_p is the photocurrent, P is the illumination power, η_{ext} is the external quantum efficiency (assumed to be 10% due to ~10% of the optical absorption of MoS_2 over the visible region) [18], [23], G is the photogain, q is the electronic charge, h is Planck's constant, and ν is the frequency of the incident wavelength [30].

The photogain as a function of electrode spacing is shown in Fig. 3(b). The photogain increases due to the decrease of the carrier transition time and the reduction of the trapping probability of the photocarriers on the MoS_2 surface as decreasing electrode spacing. The typical planar MSM PDs absorb the light at the semiconductor region between interdigitated contacts on the top of the device instead of semiconductor regions under Au electrodes. When biased, the planar MSM device represents two diodes in series, one forward biased and the other reverse biased. The depletion region increases with applied voltage. In our MoS_2 PDs, the width of the depletion region W_d between Au contacts under 10 V bias is ~1 μm using $W_d \approx [2\varepsilon\varepsilon_0 V/qN]^{1/2}$, where $\varepsilon = 4.9$ is the relative dielectric constant, $\varepsilon_0 = 8.85 \times 10^{-14}$ F/cm is the permittivity of free space, $q = 1.6 \times 10^{-19}$ C is the electron charge, and N ($\sim 10^{-16}$cm^{-3}) is the doping concentration $= I_d/(d\mu qE)$, where I_d is the drain current density, d is the channel width, μ is the field-effect mobility of electrons, and E is the electric field in the channel [31]–[33]. It is important to have metal interdigitated fingers with finger spacing as small as possible for increasing the ratio of the depletion region to the active region to achieve a large responsivity. This is because the photocarriers generated within the depleted region will give rise to a drift current while the photocarriers generated outside the depleted region and within a diffusion length will diffuse into the junction and give rise to a diffusion current.

Accordingly, MoS_2 PDs with 4-μm contact spacing exhibit superior photogain of 24 and responsivity up to 1.04 (A/W).

The photogain greater than unity in the MSM Schottky PDs has been observed previously. Photogenerated carriers drift toward the metal–semiconductor interfaces due to band bending and are then trapped at the surface state sites at the Au/MoS_2 interfaces. Note that significant surface states would be produced in the Au metal/MoS_2 interfaces due to ultralarge surface-to-volume ratio in 2-D MoS_2. This means that the depletion width and the amount of band bending (or the built-in voltage) is reduced under illumination, giving rise to the decrease in Schottky barrier height φ_b [34]–[36]. This process is described as a light-induced change in the Fermi-level partial pinning [35], [37]. According to the thermionic emission theory for MSM back-to-back Schottky diodes, φ_b ($\sim$0.54 eV) of MoS_2 PDs can be estimated by

$$I_{\rm sat} = AA^*T^2 \exp\left(-q\varphi_b/k_BT\right) \tag{3}$$

where $I_{\rm sat}$ is the saturation current, A is the area of the Schottky junction, $A^* = 4\pi qm^*(\mathrm{k}_B)^2\mathrm{h}^{-3}$ is the Richardson constant, q is the elementary charge, k_B is the Boltzmann constant, T is the temperature, m^* is the effective mass, and h is the Plank constant [37]–[40]. One should note that as MoS_2 thickness is down to a few layers, the Schottky barrier height is significantly dependent on the thickness; the layer dependence becomes insignificant as the thickness is increased. For example, Shanmugam *et al.* reported that Schottky-barrier height of Au-MoS_2 is unaltered ($\sim$1.0 eV) as the thickness of MoS_2 is higher than 100 nm [24]. As shown in the *I–V* curves in Fig. 3(c), the calculated photocurrent based on the photogain mechanism model of MSM PDs, i.e.,

$$I_{\rm photo} = \left\{\exp\left[\Delta\varphi_b\left(V\right)/k_bT\right] - 1\right\} I_{\rm dark} \tag{4}$$

where $I_{\rm photo}$ is the photocurrent, $I_{\rm dark}$ is the dark current, k_b is the Boltzmann constant, T is the temperature, and $\Delta\varphi_b(V)$ is the bias-dependent reduction of Schottky barrier height, shows a good agreement with the experimental results [37]. The $\Delta\varphi_b$ as a function of applied voltage fitted from Fig. 3(c) is shown in Fig. 3(d). As the applied bias is increased to $\sim$10 V, the $\Delta\varphi_b$ reaches its maximum value of $\sim$0.2 eV, showing a non-ideal factor of Schottky junctions [30]. Briefly speaking, under illumination, the photocarriers trapped by surface states at the metal–semiconductor interfaces lead to the reduction of the Schottky barrier height and then the production of photogain greater than unity [30], [34]–[36].

In order to investigate the radiation tolerance characteristics for harsh environment applications (e.g., space applications), the MoS_2 MSM PDs were irradiated with the 2 MeV proton fluences ranging from 10^{10} to 10^{12} cm^{-2}. Note that the protons with the energy less than 2 MeV occupy a volume of earth's space with the fluences ranging from 10^1 to 10^8 cm^{-2} (the corresponding region at geocentric distances of about 1 L–12 L, where L is approximately equal to the geocentric distance of a field line in the geomagnetic equator) [41]. Fig. 4(a) shows the $I-V$ curves of MoS_2 MSM PDs after proton irradiation measured in the dark at room temperature. The increase in dark current with proton fluence is due to the proton-induced displacement damage [42]. To quantitatively evaluate the radiation-dependent photosensing characteristics of the MoS_2 MSM PDs, the photo-to-dark current ratio (PDCR, defined as $(I_{\rm ph} - I_d)/I_d$, where $I_{\rm ph}$ is the photocurrent and I_d is the dark current) versus the proton irradiation fluence is shown in Fig. 4(b) [43]. It indicates that the MoS_2 MSM PDs are capable of photodetection even after proton irradiation exposure with the fluences of 10^{11} cm^{-2}, suggesting that the lightweight MSM PDs employing layered MoS_2 are well suited for photosensing in the space environment due to high radiation hardness of MoS_2. As the proton irradiation fluence is increased to 10^{12} cm^{-2}, the PDCR value decreases to zero, indicating that the dark current increases largely due to the huge generation of proton-induced displacement damage at high irradiation fluences, leading to the operation failure of MoS_2 MSM PDs.

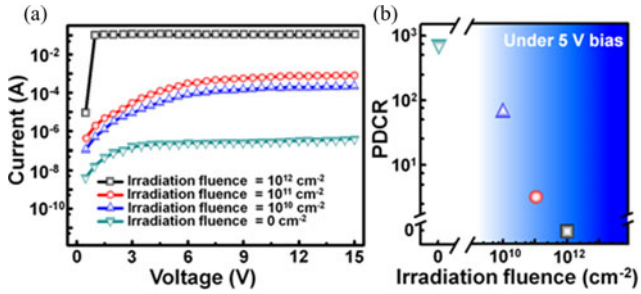

Fig. 4. (a) $I-V$ curves of the MoS_2 MSM PDs as a function of fluence of 2-MeV proton irradiation measured in the dark at room temperature. (b) PDCR value of the MoS_2 MSM PDs as function of 2-MeV proton irradiation fluence under the bias of 10 V and 532-nm light illumination ($I_{\rm light} = 2.0 \times 10^4$ W/m^2) at room temperature.

IV. Conclusion

In summary, MSM Schottky PDs employing MoS_2 trilayers exhibit the high responsivity/photogain of 1.04 (A/W)/24 and high radiation resistance for 2-MeV protons with the fluences up to $\sim 10^{11}$ cm^{-2}. Furthermore, the MoS_2 MSM PDs show ultrafast optical switch, i.e., the rise time/fall time of PDs of 40/50 μs as the contact spacing reduces to 4 μm. The photogain generation in the MoS_2 MSM Schottky PDs is attributed to the photocarriers generated at the MoS2 between two Au electrodes and trapped in the surface states at interfaces between Au/MoS_2 contacts, resulting in the enhancement of responsivity. The trilayered MoS_2 with high radiation resistance fabricated by a low-cost process holds promise for the next-generation optoelectronics in harsh environments.

References

[1] M. Chhowalla, H. S. Shin, G. Eda, L.-J. Li, K. P. Loh, and H. Zhang, "The chemistry of two-dimensional layered transition metal dichalcogenide nanosheets," *Nature Chem.*, vol. 5, pp. 263–275, 2013.

[2] K. S. Novoselov, D. Jiang, F. Schedin, T. J. Booth, V. V. Khotkevich, S. V. Morozov, and A. K. Geim, "Two-dimensional atomic crystals," *Proc. Nat. Acad. Sci. USA*, vol. 102, pp. 10451–10453, 2005.

[3] B. Radisavljevic, M. B. Whitwick, and K. Kis, "Integrated circuits and logic operations based on single-layer MoS_2," *ACS Nano*, vol. 5, pp. 9934–9938, 2005.

[4] Y.-H. Lee, L. Yu, H. Wang, W. Fang, X. Ling, Y. Shi, C.-T. Lin, J.-K. Huang, M.-T. Chang, C.-S. Chang, M. Dresselhaus, T. Palacios, L.-J. Li, and J. Kong, "Synthesis and transfer of single-layer transition metal disulfides on diverse surfaces," *Nano Lett.*, vol. 13, pp. 1852–1857, 2013.

[5] H. Ko, K. Takei, R. Kapadia, S. Chuang, H. Fang, P. W. Leu, K. Ganapathi, E. Plis, H. S. Kim, S.-Y. Chen, M. Madsen, A. C. Ford, Y.-L. Chueh, S. Krishna, S. Salahuddin, and A. Javey, "Ultrathin compound semiconductor on insulator layers for high-performance nanoscale transistors," *Nature*, vol. 468, pp. 286–289, 2010.

[6] K. S. Novoselov, V. I. Falíko, L. Colombo, P. R. Gellert, M. G. Schwab, and K. Kim, "A roadmap for graphene," *Nature*, vol. 490, pp. 192–200, 2012.

[7] F. Xia, T. Mueller, R. Golizadeh-Mojarad, M. Freitag, Y. Lin, J. Tsang, V. Perebeinos, and P. Avouris, "Photocurrent imaging and efficient photon detection in a graphene transistor," *Nano Lett.*, vol. 9, pp. 1039–1044, 2009.

[8] F. Xia, T Mueller, Y. M. Lin, A. Valdes-Garcia, and P. Avouris, "Ultrafast graphene photodetector," *Nature Nanotechnol.*, vol. 4, pp. 839–843, 2009.

[9] T. Mueller, F. Xia, and P. Avouris, "Graphene photodetectors for high-speed optical communications," *Nature Photon.*, vol. 4, pp. 297–301, 2010.

[10] F. Bonaccorso, Z. Sun, and A. C. Ferrari, "Graphene photonics and optoelectronics," *Nature Photon.*, vol. 4, pp. 611–621, 2010.

[11] Q. H. Wang, K. Kalantar-Zadeh, A. Kis, J. N. Coleman, and M. S. Strano, "Electronics and optoelectronics of two-dimensional transition metal dichalcogenides," *Nature Nanotechnol.*, vol. 7, pp. 699–712, 2012.

[12] G. Konstantatos, M. Badioli, L. Gaudreau, J. Osmond, M. Bernechea, F. P. G. de Arquer, F. Gatti, and F. H. L. Koppens, "Hybrid graphene–quantum dot phototransistors with ultrahigh gain," *Nature Nanotechnol.*, vol. 7, pp. 363–368, 2012.

[13] T. J. Echtermeyer, L. Britnell, P. K. Jasnos, A. Lombardo, R. V. Gorbachev, A. N. Grigorenko, A. K. Geim, A. C. Ferrari, and K. S. Novoselov, "Strong plasmonic enhancement of photovoltage in graphene," *Nature Commun.*, vol. 2, pp. 458-1–458-5, 2011.

[14] Y. Liu, R. Cheng, L. Liao, H. Zhou, J. Bai, G. Liu, L. Liu, Y. Huang, and X. Duan, "Plasmon resonance enhanced multicolour photodetection by graphene," *Nature Commun.*, vol. 2, pp. 579-1–579-7, 2011.

[15] M. Furchi, A. Urich, A. Pospischil, G. Lilley, K. Unterrainer, H. Detz, P. Klang, A. M. Andrews, W. Schrenk, G. Strasser, and T. Mueller, "Microcavity-integrated graphene photodetector," *Nano Lett.*, vol. 12, pp. 2773–2777, 2012.

[16] B. Radisavljevic, A. Radenovic, J. Brivio, V. Giacometti, and A. Kis, "Single-layer MoS_2 transistors," *Nature Nanotechnol.*, vol. 6, pp. 147–150, 2012.

[17] Y. Zhang, J. Ye, Y. Matcuhashi, and Y. Iwasa, "Ambipolar MoS_2 thin flake transistors," *Nano Lett.*, vol. 12, pp. 1136–1140, 2012.

[18] K. F. Mak, C. Lee, J. Hone, J. Shan, and T. F. Heinz, "Atomically thin MoS_2: A new direct-gap semiconductor," *Phys. Rev. Lett.*, vol. 105, pp. 136805-1–136805-4, 2010.

[19] K. K. Liu, W. Zhang, Y. H. Lee, Y. C. Lin, M. T. Chang, C. Y. Su, C. S. Chang, H. Li, Y. Shi, H. Zhang, C. S. Lai, and L. J. Li, "Growth of large-area and highly crystalline MoS_2 thin layers on insulating substrates," *Nano Lett.*, vol. 12, pp. 1538–1544, 2012.

[20] G. Eda, H. Yamaguchi, D. Voiry, T. Fujita, M. Chen, and M. Chhowalla, "Photoluminescence from chemically exfoliated MoS_2," *Nano Lett.*, vol. 11, pp. 5111–5116, 2011.

[21] W. Choi, M. Y. Cho, A. Konar, J. H. Lee, G. B. Cha, S. C. Hong, S. Kim, J. Kim, D. Jean, J. Joo, and S. Kim, "High-detectivity multilayer MoS_2 phototransistors with spectral response from ultraviolet to infrared," *Adv. Mater.*, vol. 24, pp. 5832–5836, 2012.

[22] H. S. Lee, S. W. Min, Y. G. Chang, M. K. Park, T. Nam, H. Kim, J. H. Kim, S. Ryu, and S. Im, "MoS_2 nanosheet phototransistors with thickness-modulated optical energy gap," *Nano Lett.*, vol. 12, pp. 3695–3700, 2012.

[23] D. S. Tsai, K. K. Liu, D. H. Lien, M. L. Tsai, C. F. Kang, C. A. Lin, L. J. Li, and J. H. He, "Few layer MoS_2 with broadband high photogain and fast optical switching for use in harsh environments," *ACS Nano*, vol. 7, pp. 3905–3911, 2013.

[24] M. Shanmugam, C. A. Durcan, and B. Yu, "Layered semiconductor molybdenum disulfide nanomembrane based Schottky-barrier solar cells," *Nanoscale*, vol. 4, pp. 7399–7405, 2012.

[25] R. S. Sundaram, M. Engle, A. Lombardo, R. Krupke, A. C. Ferrari, Ph. Avouris, and M. Steiner, "Electroluminescence in single layer MoS_2," *Nano Lett.*, vol. 13, pp. 1416–1421, 2013.

[26] Z. Yin, H. Li, H. Li, L. Jiang, Y. Shi, Y. Sun, G. Lu, Q. Zhang, X. Chen, and H. Zhang, "Single-layer MoS_2 phototransistors," *ACS Nano*, vol. 6, pp. 74–80, 2012.

[27] M. A. Xapsos, G. P. Summers, J. L. Barth, E. G. Stassinopoulos, and E. A. Burke, "Probability model for worst case solar proton event fluences," *IEEE Trans. Nucl. Sci.*, vol. 46, pp. 1481–1485, 1999.

[28] C. Barenes, G. Swift, A. Johnston, B. Rax, and K. LaBel, "Radiation effects considerations for the application of photonics in space systems," *IEEE Aerosp. Conf.*, vol. 2, pp. 219–239, 1998.

[29] S. Y. Chou, Y. Liu, and P. B. Fisher, "Tera-hertz GaAs metal–semiconductor–metal photodetectors with 25 nm finger spacing and finger width," *Appl. Phys. Lett.*, vol. 61, pp. 477–479, 1992.

[30] Q. Yang, X. Guo, W. Wang, Y. Zhang, S. Xu, D. H. Lien, and Z. L. Wang, "Enhancing sensitivity of a single ZnO micro-/nanowire photodetector by piezo-phototronic effect," *ACS Nano*, vol. 10, pp. 6285–6291, 2010.

[31] S. M. Sze, D. J. Coleman Jr., and A. Loya, "Current transport in metal–semiconductor–metal (MSM) structure," *Solid-State Electron.*, vol. 14, pp. 1209–1218, 1971.

[32] W. Kautek, H. Gerischer, and H. Tributsch, "The role of carrier diffusion and indirect optical transitions in the photoelectrochemical behavior of layer type d-band semiconductors," *J. Electrochem. Soc.*, vol. 127, pp. 2471–2478, 1980.

[33] T. Ytterdal, Y. Cheng, and T. A. Fjeldly, *Device Modeling for Analog and RF CMOS Circuit Design*. New York, NY, USA: Wiley, 2003.

[34] R. R. Mehta and B. S. Sharma, "Photoconductive gain greater than unity in CdSe films with Schottky barriers at contacts," *J. Appl. Phys.*, vol. 44, pp. 325–328, 1973.

[35] O. Katz, V. Garber, B. Meyler, G. Bahir, and J. Salzman, "Gain mechanism in GaN Schottky ultraviolet detectors," *Appl. Phys. Lett.*, vol. 79, pp. 1417–1419, 2001.

[36] M. Klingenstein, J. Kuhl, J. Rosenzweig, C. Moglestue, A. Hülsmann, J. Schneider, and K. Köhler, "Photocurrent gain mechanisms in metal–semiconductor–metal photodetectors," *Solid-State Electron.*, vol. 37, pp. 333–340, 1994.

[37] S. M. Sze and K. K. Ng, *Physics of Semiconductor Devices*. Hoboken, NJ, USA: Wiley, 2007.

[38] W. J. Yu, Z. Li, H. Zhou, Y. Chen, Y. Wang, Y. Huang, and X. Duan, "Vertically stacked multi-heterostructures of layered materials for logic transistors and complementary inverters," *Nature Mater.*, vol. 12, pp. 246–252, 2013.

[39] E. S. Kadantsev and P. Hawrylak, "Electronic structure of a single MoS_2 monolayer," *Solid State Commun.*, vol. 152, pp. 909–913, 2012.

[40] D. Walker and M. Razeghi, "The development of nitird-based UV photodetectors," *Opto-Electron. Rev.*, vol. 8, pp. 25–42, 2000.

[41] E. G. Stassinopoulos and J. P. Raymond, "The space radiation environment for electronics," *Proc. IEEE*, vol. 76, no. 11, pp. 1423–1442, 1988.

[42] A. Kalavagunta, A. Touboul, L. Shen, R. D. Schrimpf, R. A. Reed, D. M. Fleetwood, R. K. Jain, and U. K. Mishra, "Electrostatic mechanisms responsible for device degradation in AlGaN/AlN/GaN HEMTs," *IEEE Trans. Nucl. Sci.*, vol. 55, pp. 2106–2112, 2008.

[43] D. S. Tsai, C. F. Kang, H. H. Wang, C. A. Lin, J. J. Ke, Y. H. Chu, and J. H. He, "n-ZnO/$LaAlO_3$/p-Si heterojunction for visible-blind UV detection," *Opt. Lett.*, vol. 37, pp. 1112–1114, 2012.

Dung-Sheng Tsai received the Ph.D. degree from the Graduate Institute of Photonics and Optoelectronics, National Taiwan University, Taipei, Taiwan, in 2012. He is currently a Postdoctoral Fellow in the Graduate Institute of Photonics and Optoelectronics, National Taiwan University. His current research interests include photo sensors, photoelectronic devices based on nanomaterials.

Der-Hsien Lien received the B.S. and M.S. degrees from the National Tsing Hua University, Hsinchu, Taiwan. He is currently working toward the Ph.D. degree at the Graduate Institute of Electronics, National Taiwan University, Tapei, Taiwan.

Meng-Lin Tsai received the B.S. degree from the National Tsing Hua University, Hsinchu, Taiwan. He is currently with the Department of Electrical Engineering, and Graduate Institute of Photonics and Optoelectronics, National Taiwan University, Taipei, Taiwan.

Sheng-Han Su received the B.S. degree from the Chang Gung University, Taoyuan, Taiwan, in 2010 and the M.S. degree from the Institute of Nanotechnology and Microsystem Engineer, National Cheng Kung University, Tainan, Taiwan, in 2012. She is currently with the Department of Electrical Engineering, and Graduate Institute of Photonics and Optoelectronics, National Taiwan University, Taipei, Taiwan.

Kuan-Ming Chen received the M.S. degree from the Graduate Institute of Electronics Engineering, National Taiwan University, Taipei, Taiwan, in 2005. He is currently a Technical Staff member at the Tandem Accelerator Lab, Institute of Physics, Academia Sinica, Taipei, Taiwan, since 1994.

Jr-Jian Ke received the B.S. degree in electrical engineering from the National University of Kaohsiung, Kaohsiung ,Taiwan, in 2007 and the M.S. degree from the Graduate Institute of Photonics and Optoelectronics, National Taiwan University, Taipei, Taiwan, in 2009, where he is currently working toward the Ph.D. degree. His past research actives include the transport mechanism of nanowires and metal–semiconductor interface. He is currently working on the fabrication, transport modeling of the resistive random-access memory devices and their applications.

Yueh-Chung Yu received the Ph.D. degree from the University of North Texas, Denton, TX, USA, in 1991. He is currently an Associate Research Fellow in the Institute of Physics, Academia Sinica, Taipei, Taiwan. His research interests are focused on the ion-solid interaction, Rutherford backscattering, particle induced X-ray emission, and ion irradiation.

Lain-Jong Li received the B.Sc. and M.Sc. degrees in chemistry from the National Taiwan University. After 5 years of R&D at the Taiwan Semiconductor Manufacturing Company, he received the Ph.D. degree in condensed matter physics from Oxford University, U.K., in 2006. He was an Assistant Professor in the School of Materials Science and Engineering, Nanyang Technical University, Singapore. Since 2010, he has been an Associate Research fellow at Academia Sinica Taiwan. He received Humboldt Research Fellowship for Experienced Researchers (Germany) and Career Development Award (Academia Sinica, Taiwan), respectively, in 2011 and 2010. His current research interests include 1) Growth and characterization of 2-D materials including graphene and its analog such as Mos_2 and WS_2. 2) Energy-related applications based on 2-D materials, such as energy storage, hydrogen generation, and low-power electronics.

Jr-Hau He (SM'13) received the Ph.D. degree from the National Tsing Hua University, Hsinchu, Taiwan, in 2005. He is currently an Associate Professor in the Department of Electrical Engineering, Graduate Institute of Photonics and Optoelectronics, National Taiwan University, Taipei, Taiwan. He is involved in the designing of new nanostructured architectures for nanophotonics and the next generation of nanodevices, including photovoltaics, and resistive memory. He has been recognized internationally. He serves as a referee for numerous prestigious journals, and the Chair, the Co-chair, and a committee member for national and international symposiums. He received the the Outstanding Youth Award of Taiwan Association for Coating and Thin Film Technology (2012), the Youth Optical Engineering Medal of Taiwan Photonics Society (2011), the Distinguished Young Researcher Award of the Electronic Devices and Materials Association (2011), the Prof. Jiang Novel Materials Youth Prize of International Union of Pure and Applied Chemistry (IUPAC) (2011), and the Exploration Research Award of Pan Wen Yuan Foundation (2008) and selected as a Member of the Global Young Academy (2011), and has won a lot of awards and honors with his students in professional societies and conferences in Taiwan and internationally. The laboratory has graduated 2 Ph.D. and 22 M.S. alumni to date.